

FIB-SEM tomography of human skin telocytes and their extracellular vesicles

Dragos Cretoiu ^{a, b}, Mihaela Gherghiceanu ^b, Eric Hummel ^c, Hans Zimmermann ^c,
Olga Simionescu ^d, Laurentiu M. Popescu ^{a, b, *}

^a Department of Cellular and Molecular Medicine, Carol Davila University of Medicine and Pharmacy, Bucharest, Romania

^b Victor Babeş National Institute of Pathology, Bucharest, Romania

^c Carl Zeiss Microscopy, GmbH, Munich, Germany

^d Department of Dermatology, Colentina University Hospital, Carol Davila University of Medicine and Pharmacy, Bucharest, Romania

Received: December 9, 2014; Accepted: February 15, 2015

Abstract

We have shown in 2012 the existence of telocytes (TCs) in human dermis. TCs were described by transmission electron microscopy (TEM) as interstitial cells located in non-epithelial spaces (stroma) of many organs (see www.telocytes.com). TCs have very long prolongations (tens to hundreds micrometers) named Telopodes (Tps). These Tps have a special conformation with dilated portions named podoms (containing mitochondria, endoplasmic reticulum and caveolae) and very thin segments (below resolving power of light microscopy), called podomers. To show the real 3D architecture of TC network, we used the most advanced available electron microscope technology: focused ion beam scanning electron microscopy (FIB-SEM) tomography. Generally, 3D reconstruction of dermal TCs by FIB-SEM tomography revealed the existence of Tps with various conformations: (i) long, flattened irregular veils (ribbon-like segments) with knobs, corresponding to podoms, and (ii) tubular structures (podomers) with uneven calibre because of irregular dilations (knobs) – the podoms. FIB-SEM tomography also showed numerous extracellular vesicles (diameter 438.6 ± 149.1 nm, $n = 30$) released by a human dermal TC. Our data might be useful for understanding the role(s) of TCs in intercellular signalling and communication, as well as for comprehension of pathologies like scleroderma, multiple sclerosis, psoriasis, etc.

Keywords: dermis • FIB-SEM tomography • telocytes • telopodes • extracellular vesicles • scleroderma • multiple sclerosis

Introduction

Telocytes (TCs) were described 5 years ago [1] as a new cell type in the interstitial space of many organs [2–23] as well as in human skin [24] (see www.telocytes.com). Their presence in human dermis was confirmed [18, 25–27] and their importance for pathology was revealed [28–35]. The main differential diagnosis of TCs in human papillary dermis should be made with fibroblasts. Indeed, numerous data suggested there are a lot of differences between TCs and fibroblasts: (i) the aspect of TCs and fibroblasts is not the same in tissue culture [36, 37]; (ii) transmission electron microscopy (TEM) shows completely different ultrastructure, e.g. [5, 18, 20, 38]; (iii) microRNA imprint is dissimilar, e.g. [39]; (iv) gene profile are not the same [40–42] and (v) proteomics showed striking differences [43].

Focused ion beam scanning electron microscopy (FIB-SEM) is now the election technique for three-dimensional (3D) visualization of biological structures (cells) at nanoscale resolution [44–53]. FIB-SEM tomography allows 3D imaging at the subcellular level and is considered a breakthrough for ultrastructural volume reconstruction.

Here, we present FIB-SEM tomography of human papillary dermis TCs showing their complex 3D architecture, as well as the budding and shedding of extracellular vesicles. FIB-SEM tomography does not contradict TEM, but provides additional important details.

Material and methods

Sample preparation

Biopsies of human skin were obtained from three patients (informed written consent). Normal skin samples were obtained from a re-excision

*Correspondence to: LAURENTIU M. POPESCU, M.D., Ph.D.,
Department of Cellular and Molecular Medicine, Carol Davila University
of Medicine and Pharmacy, Bucharest, Romania.
E-mail: LMP@jcmm.org

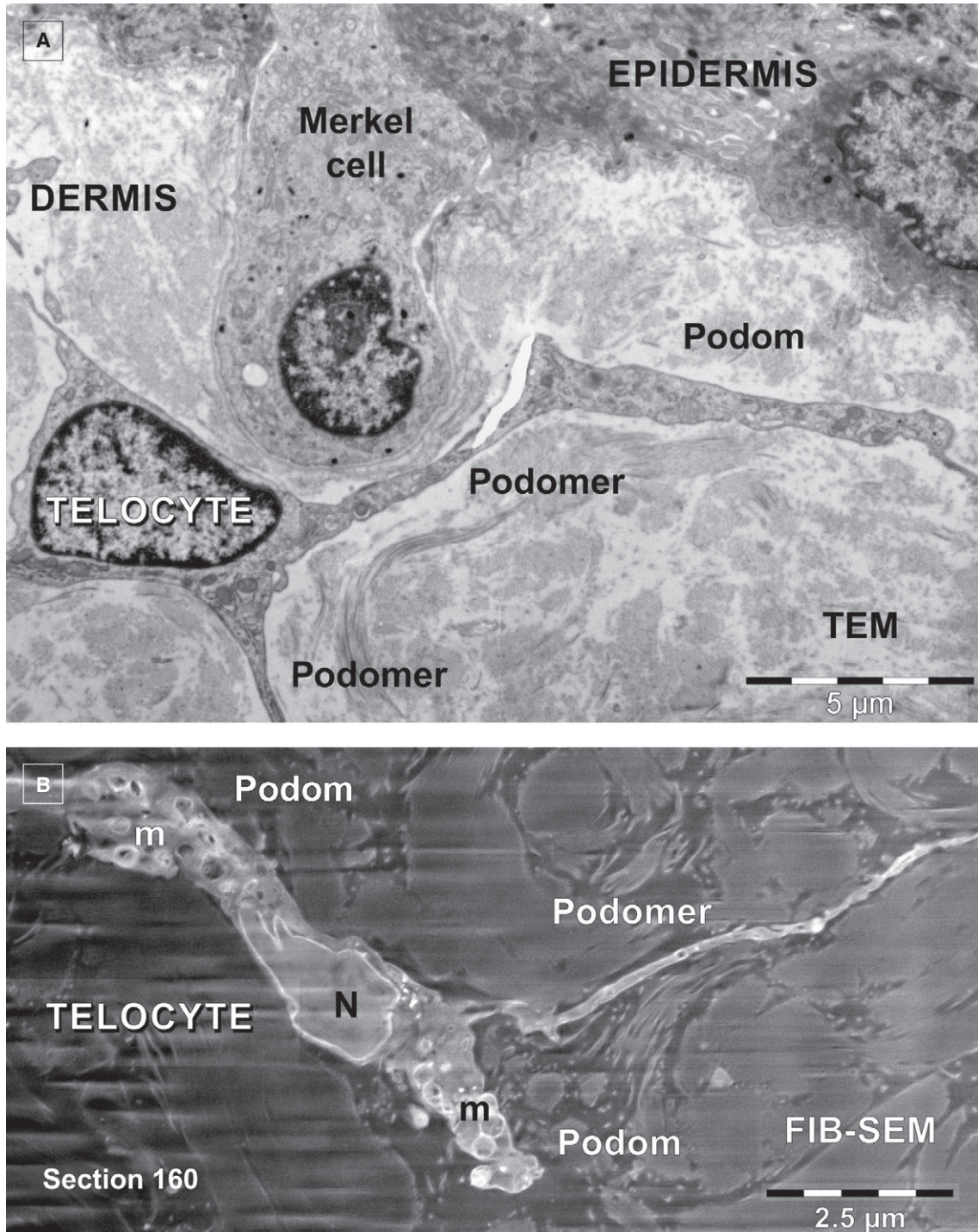


Fig. 1 (A and B) Telocytes in human papillary dermis. (A) Transmission electron microscopy shows a telocyte with 3 telopodes edging a Merkel cell. (B) FIB-SEM backscattered electron imaging mode shows a telocyte with two telopodes in dermis.

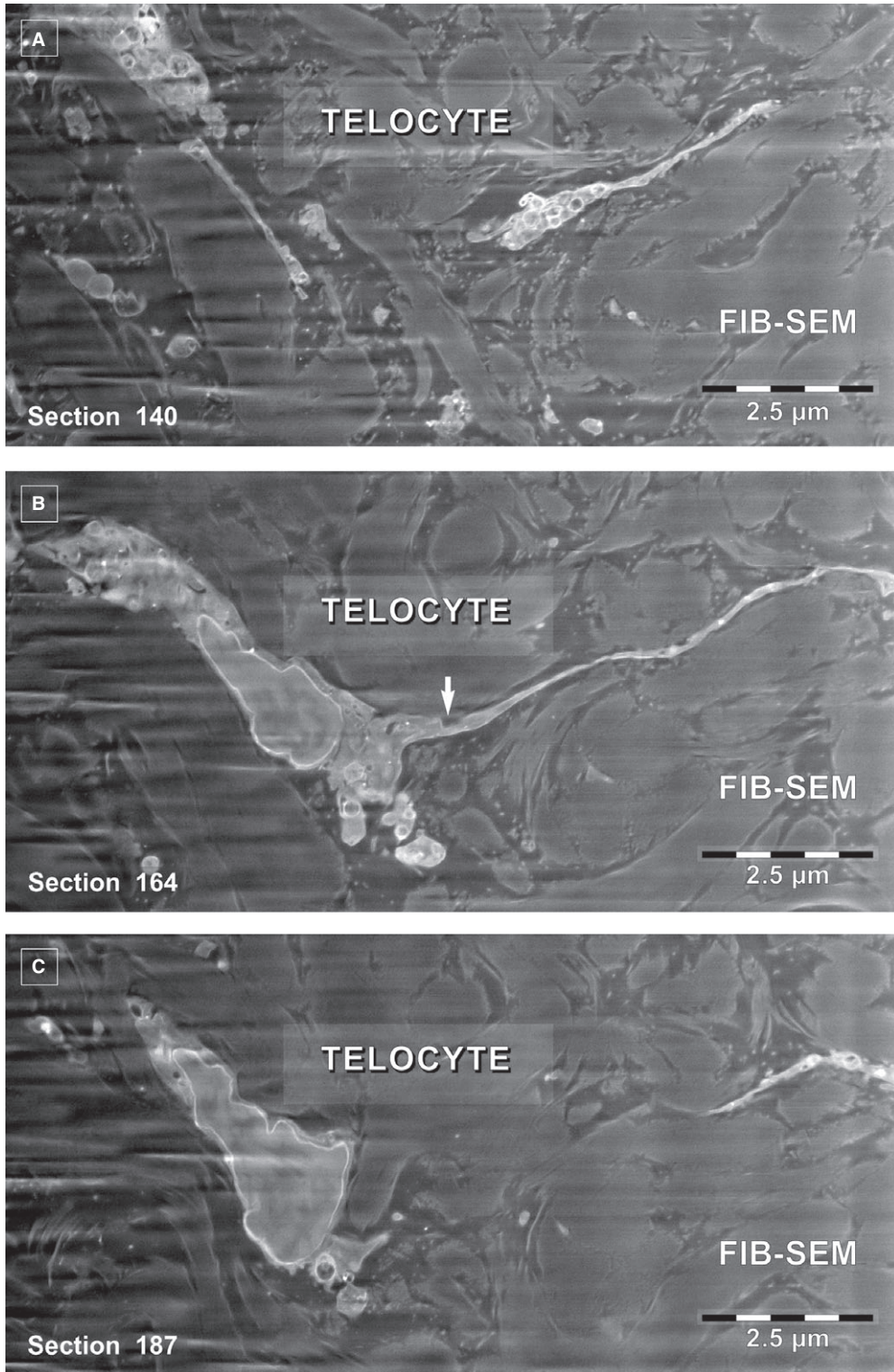


Fig. 2 (A–C) FIB-SEM backscattered electron images. Three non-consecutive serial images obtained at $\sim 1.2 \mu\text{m}$ z-interval show the narrow emergence (arrow) of a telopode from the cellular body of a telocyte.

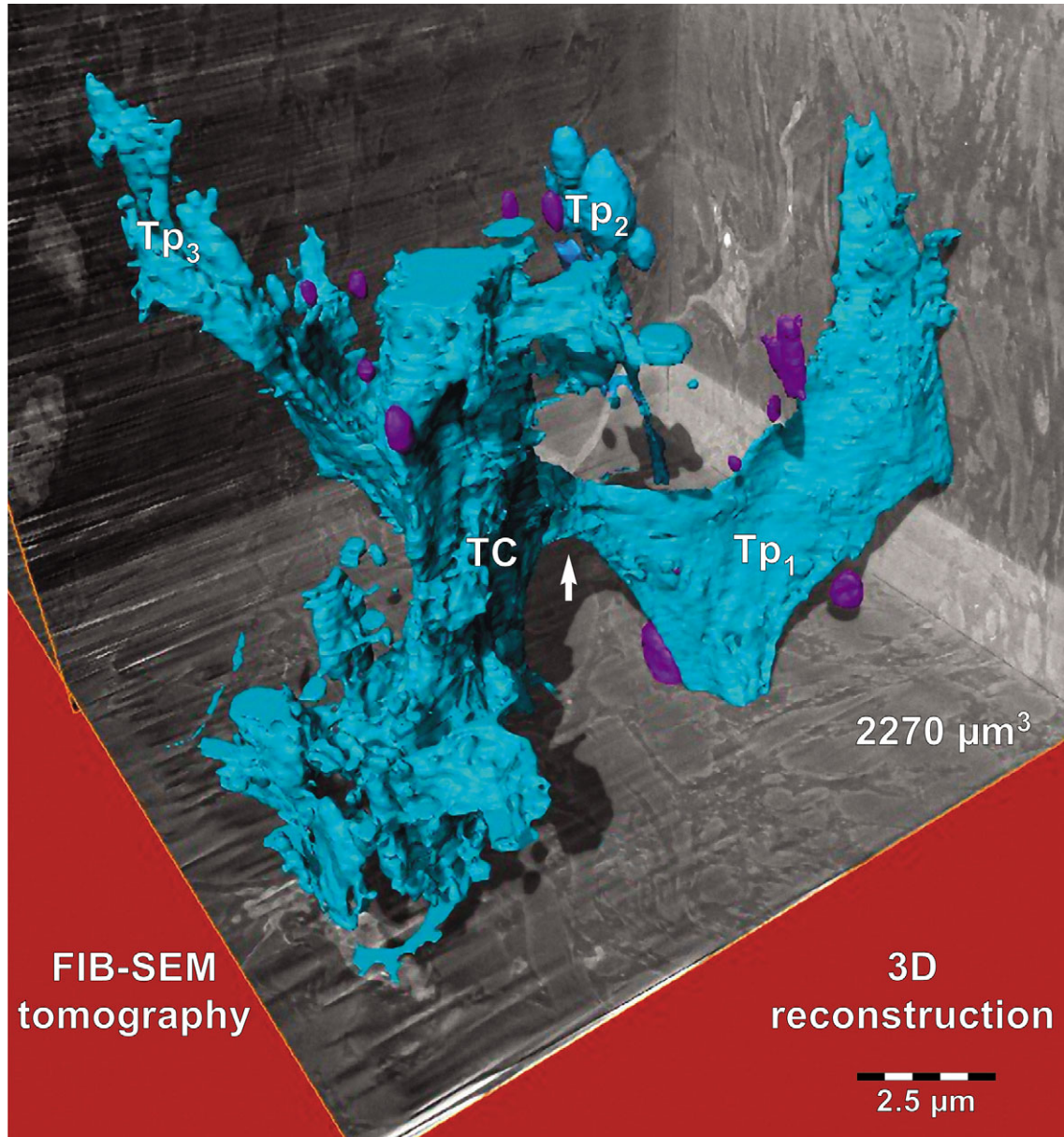


Fig. 3 FIB-SEM tomography of a $2270 \mu\text{m}^3$ volume from human papillary dermis encompasses a segment from a telocyte reconstructed in blue. Three dimensional reconstruction of the stack containing the telocyte shows a ‘wing-like’ telopode (Tp1), a telopode (Tp2) with typical appearance (details in Fig. 4) and a telopode (Tp3) with anfractuouse contour. The arrow indicates the narrow emergence of Tp1 suggested by serial imaging in Figure 2. A portion of the cell body (TC) is located in the centre. At least 10 extracellular vesicles appear reconstructed in purple.

procedure after removing a local melanoma. The second excisions were performed according to the Breslow index (tumoural depth), 14 days after primary excision. The samples of normal skin were taken at 1-cm distance from primary suture [24]. Experiments were performed according to the Helsinki guidelines, in full compliance with the Bioethics Committee of the ‘Victor Babeş’ National Institute of Pathology, Bucharest regulations. The small samples of skin were processed as

described previously [12]. Briefly, the 1-mm-cube fragments were fixed by immersion in 4% glutaraldehyde, and post-fixed in 1% OsO_4 with 1.5% $\text{K}_4\text{Fe}(\text{CN})_6$ (potassium ferrocyanide – reduced osmium) to increase the membranes contrast. Subsequently, the samples were dehydrated through increasing graded ethanol series and embedded in epoxy resin (Agar 100 from Agar Scientific, Essex, UK) at 60°C for 48 hrs.

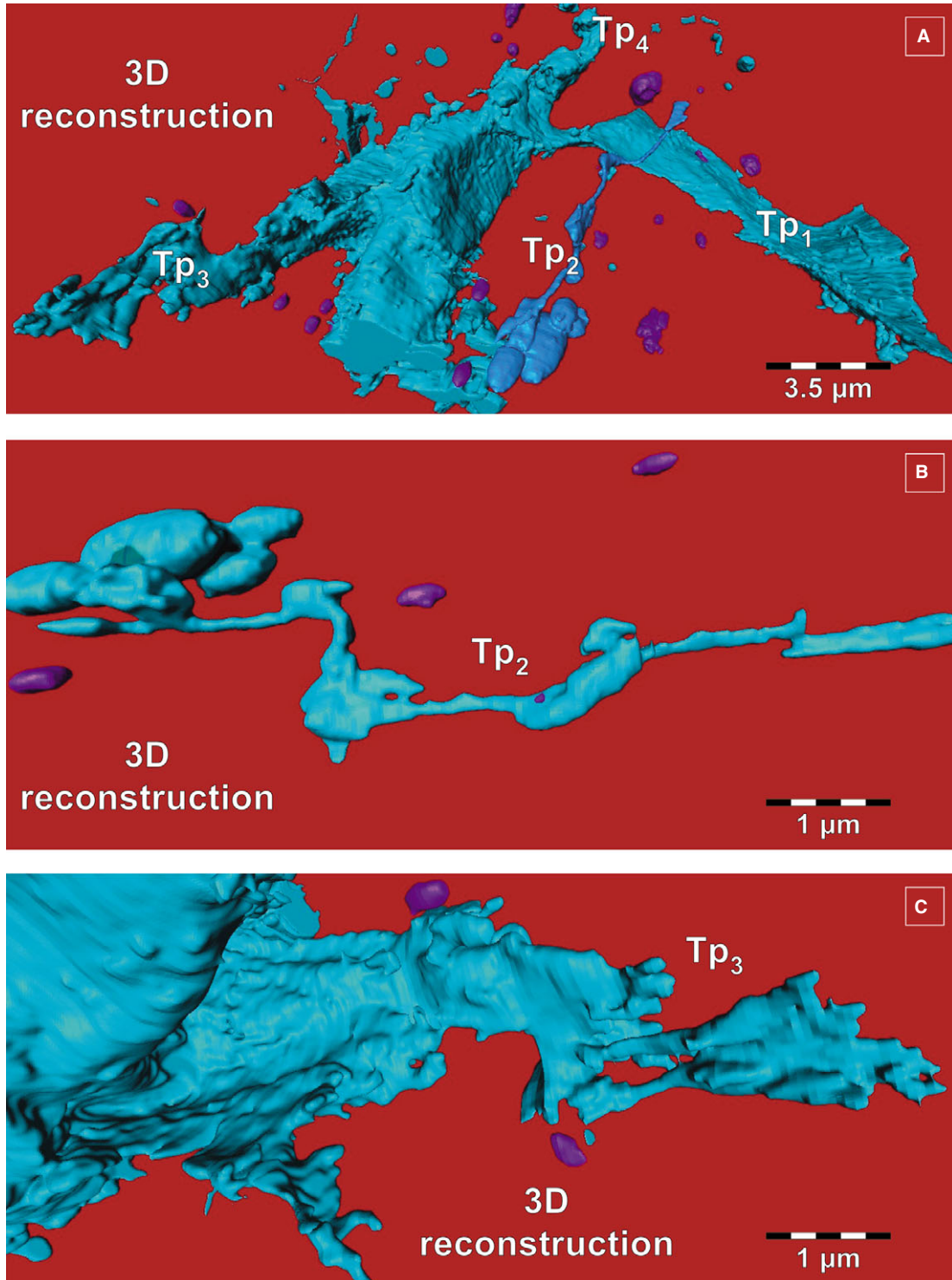


Fig. 4 (A–C) FIB-SEM tomography. Three dimensional reconstruction details of telopodes from Figure 3, from different viewing angles. **(A)** From this angle, a fourth telopode (Tp4) can be seen. **(B)** Tp2 from Figure 3 has enlarged segments (podoms) alternating with slender segments. **(C)** Telopode (Tp3 from Fig. 3) with anfractuous contour. Extracellular vesicles appear in purple.

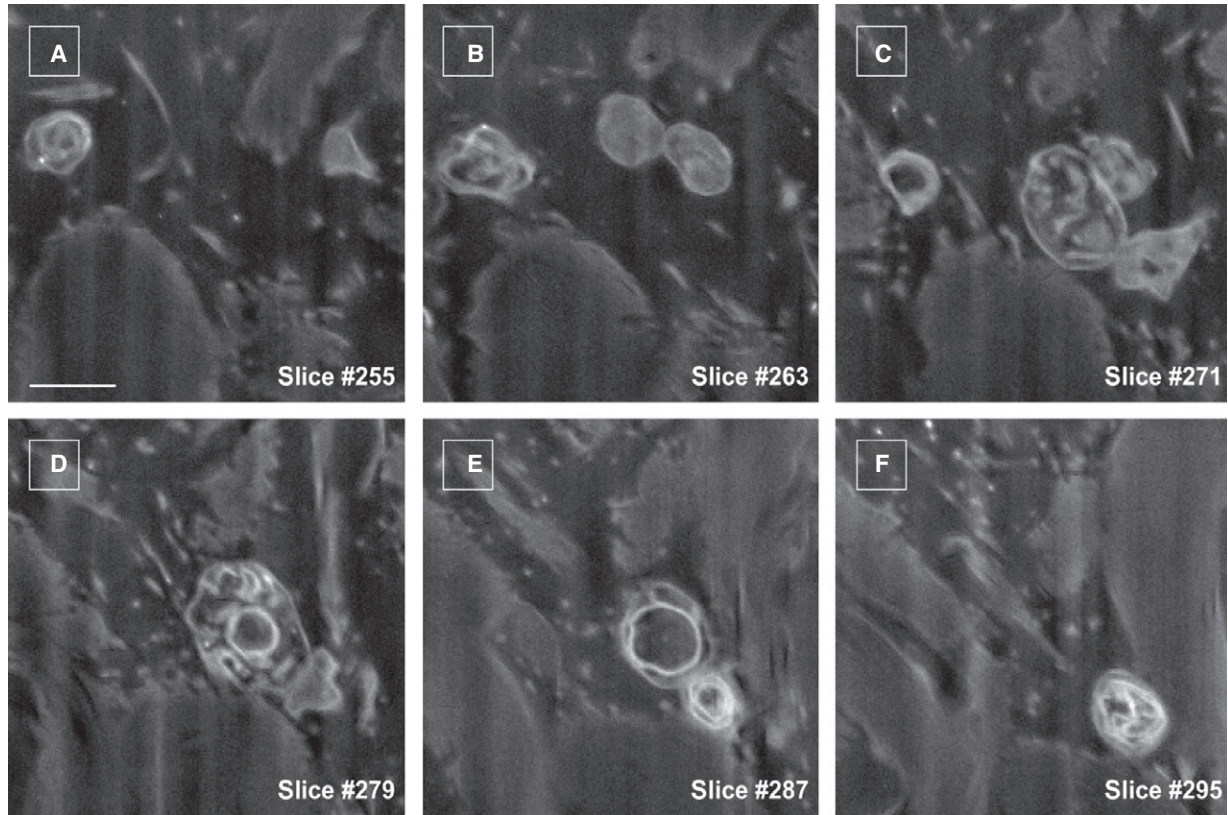


Fig. 5 FIB-SEM of extracellular vesicles dynamics around a telocyte. Scale bar is 0.5 μm .

FIB/SEM image stack acquisition

Focused ion beam milling and SEM imaging were carried out with a ZEISS Auriga Crossbeam system (from Carl Zeiss Microscopy, München, Germany). FIB milling was performed with 600 pA to 20 nA for the

given samples. SEM-Imaging current was 220 pA. To achieve the best signal contrast, the mixed Inlens and energy-selective backscattered detector signals were used. FIB milling steps was 10 nm/slice and each 5th slice was imaged. Accordingly, each image represents 50 nm of the stack, at 9k \times magnification. Image pixel size was 10.27 nm.

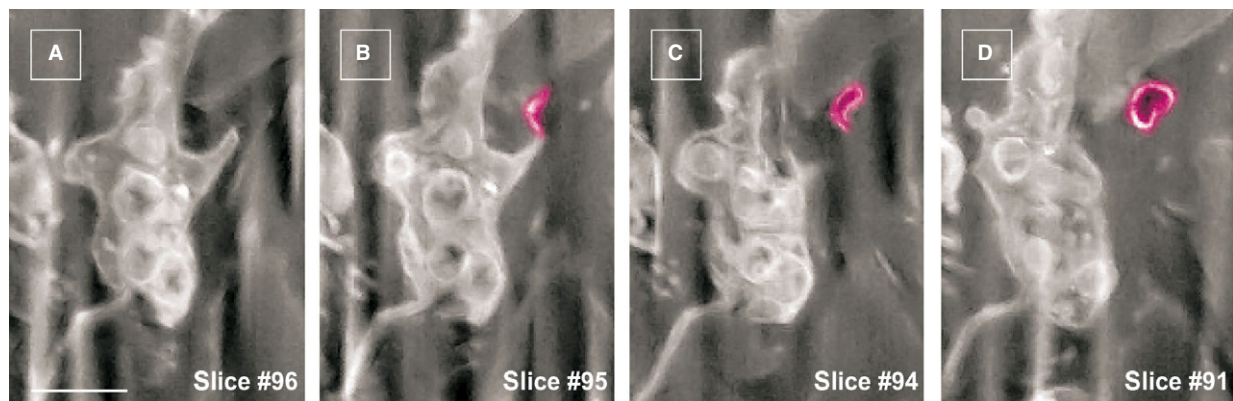


Fig. 6 FIB-SEM of a human dermal telocyte presenting an extracellular vesicle (purple) budding from a podom. Note the empty appearance of the vesicle content. Scale bar is 0.5 μm .

Image processing and analysis

Image stack was analyzed and processed using Adobe Photoshop CS5 Extended (Adobe Systems Incorporated, San Jose, CA, USA) for noise detection and removal and luminance level adjustment. Output images were then loaded into Amira 5.0.1 (Visage Imaging, Berlin, Germany) software package. Structures of interest were manually segmented and reconstructed. Stacks of images were also loaded in VirtualDub v1.10.4 (Lee A.) software as sequence of numbered JPEG files and converted to video file. Adobe Photoshop CS5 Extended was also used for vesicles 2D morphometry. Measurements were then statistically analyzed using Microsoft Excel 2013 Analysis ToolPak module.

Results and discussion

The specific morphological features of human dermal TCs are the telopodes, as demonstrated previously using TEM [24]. Figure 1A depicts a TC from the papillary dermis situated just beneath the basement membrane of epidermis in close proximity with a Merkel cell. This 2D image reveals the 'classic' morphology of a TC: a stellate body and very thin and narrow TPs, some which appear discontinuous because of the limitations of a single plane of section. For this reason, FIB-SEM technology (ZEISS Auriga Crossbeam system) was used, which allowed imaging of several hundred serial sections and accurate reconstruction of the TC 3D volume. Automated serial sectioning and imaging of human dermis provided a total of 350 micrographs. Sixty-six images were serially removed from the block face. A stack of 275 serial images (Fig. 2) were assembled to obtain a 3D reconstruction, 360° orthogonal rotation and a 3D digitally- coloured volume rendering of the TC in dermis. FIB-SEM images from Figure 2 revealed the presence of a typical TC in human dermis. The same cell was clearly visible from section 67–342 allowing the reconstruction of 2270 μm^3 (Fig. 3). The TC appearance shows a cell with different extensions: a 'ribbon-like' telopode, a telopode with classical morphology and a telopode with anfractuous shape (details in Fig. 4).

The surface-to-volume ratio is increased several folds in flat Tps compared to tubular Tps. This means, *inter alia*, a larger surface for receiving signals from extracellular space or *vice versa*. Interestingly, the dynamics of telopodes in cell culture depend on the extracellular type of matrix proteins. The stronger adherence and spreading were noted for TC seeded on fibronectin, while the lowest were on laminin [54]. Moreover, in cell cultures, low-level laser stimulation (using neodymium-doped yttrium aluminium garnet laser) determines a maximum growth rate of Tp lateral extensions of $10.3 \pm 1.0 \mu\text{m}/\text{min}$. [55]. This raises the possibility of using low-level laser stimulation for therapeutic purposes.

The 3D reconstruction by FIB-SEM tomography of human dermal TCs allowed also the identification of extracellular vesicles (Figs. 3–6, Video S1), as shown previously for cardiac TCs [56].

References

1. Popescu LM, Fausone-Pellegrini MS. TELOCYTES - a case of serendipity: the winding way from Interstitial Cells of Cajal (ICC), via Interstitial Cajal-Like Cells (ICLC) to TELOCYTES. *J Cell Mol Med*. 2010; 14: 729–40.
2. Popescu LM, Gherghiceanu M, Suciuc LC, et al. Telocytes and putative stem cells in the lungs: electron microscopy, electron

In fact, a rough estimation of the number of extracellular vesicles ($n = 30$ for one cell) showed a vesicle diameter of $438.6 \pm 149.1 \text{ nm}$. Considering the international standards *e.g.* (i) dimensions over 100 nm, (ii) origin by budding and shedding of plasma membrane and (iii) the monovesicular ultrastructure) [57, 58], we think that the extracellular vesicles we found by FIB-SEM are microvesicles or ectovesicles or shed vesicles, rather than exosomes.

As previously shown, TCs were found in human dermis having a strategic position: around blood vessels, in the perifollicular sheath, outside the glassy membrane and surrounding sebaceous glands, arrector pili muscles and both the secretory and excretory segments of eccrine sweat glands [24]. Moreover, TCs frequently co-exist in close contacts with stem cells, for example, in skin dermis [24], lungs [2], skeletal muscle [59], meninges and choroid plexus [4] or liver [7]. Therefore, we consider that TCs together stem cells form a structural and functional unit, a 'tandem' [18]. This opinion is supported by the fact that TCs transfer extracellular vesicles loaded with microRNAs to stem cells [21], as well as the fact that extracellular vesicles have potential roles in regenerative medicine [60].

Last but not least, very recent data suggest that TCs through their Tps could be regarded as a primitive nervous system [61] or being involved in morphogenetic bioelectrical signalling [62, 63]. Telocytes are expected to contribute to age-intervention protocols [64].

Acknowledgements

This project was supported by a grant of the Romanian National Authority for Scientific Research, CNCS–UEFISCDI, project number 194/2014. This article is partially supported (for D Cretoiu) by the Sectorial Operational Programme Human Resources Development (SOPHRD), financed by the European Social Fund and the Romanian Government under the contract number POSDRU/159/1.5/S/141531.

Conflicts of interest

The authors confirm that there are no conflicts of interest.

Supporting information

Additional Supporting Information may be found in the online version of this article:

Video S1. Movie presenting a vesicle budding from a podom.

- tomography and laser scanning microscopy. *Cell Tissue Res.* 2011; 345: 391–403.
3. **Cretoiu D, Cretoiu SM, Simionescu AA, et al.** Telocytes, a distinct type of cell among the stromal cells present in the lamina propria of jejunum. *Histol Histopathol.* 2012; 27: 1067–78.
 4. **Popescu BO, Gherghiceanu M, Kostin S, et al.** Telocytes in meninges and choroid plexus. *Neurosci Lett.* 2012; 516: 265–9.
 5. **Gherghiceanu M, Popescu LM.** Cardiac telocytes - their junctions and functional implications. *Cell Tissue Res.* 2012; 348: 265–79.
 6. **Luesma MJ, Gherghiceanu M, Popescu LM.** Telocytes and stem cells in limbus and uvea of mouse eye. *J Cell Mol Med.* 2013; 17: 1016–24.
 7. **Xiao J, Wang F, Liu Z, et al.** Telocytes in liver: electron microscopic and immunofluorescent evidence. *J Cell Mol Med.* 2013; 17: 1537–42.
 8. **Cretoiu SM, Cretoiu D, Marin A, et al.** Telocytes: ultrastructural, immunohistochemical and electrophysiological characteristics in human myometrium. *Reproduction.* 2013; 145: 357–70.
 9. **Bosco C, Diaz E, Gutierrez R, et al.** Ganglionar nervous cells and telocytes in the pancreas of *Octodon degus*: extra and intrapancreatic ganglionar cells and telocytes in the degus. *Auton Neurosci.* 2013; 177: 224–30.
 10. **Chen X, Zheng Y, Manole CG, et al.** Telocytes in human oesophagus. *J Cell Mol Med.* 2013; 17: 1506–12.
 11. **Diaz-Flores L, Gutierrez R, Saez FJ, et al.** Telocytes in neuromuscular spindles. *J Cell Mol Med.* 2013; 17: 457–65.
 12. **Cretoiu D, Hummel E, Zimmermann H, et al.** Human cardiac telocytes: 3D imaging by FIB-SEM tomography. *J Cell Mol Med.* 2014; 18: 2157–64.
 13. **Vannucchi MG, Traini C, Guasti D, et al.** Telocytes subtypes in human urinary bladder. *J Cell Mol Med.* 2014; 18: 2000–8.
 14. **Yang Y, Sun W, Wu SM, et al.** Telocytes in human heart valves. *J Cell Mol Med.* 2014; 18: 759–65.
 15. **Li H, Zhang H, Yang L, et al.** Telocytes in mice bone marrow: electron microscope evidence. *J Cell Mol Med.* 2014; 18: 975–8.
 16. **Galiger C, Kostin S, Golec A, et al.** Phenotypical and ultrastructural features of Oct4-positive cells in the adult mouse lung. *J Cell Mol Med.* 2014; 18: 1321–33.
 17. **Li H, Lu S, Liu H, et al.** Scanning electron microscope evidence of telocytes in vasculature. *J Cell Mol Med.* 2014; 18: 1486–9.
 18. **Cretoiu SM, Popescu LM.** Telocytes revisited. *Biomol Concepts.* 2014; 5: 353–69.
 19. **Li L, Lin M, Li L, et al.** Renal telocytes contribute to the repair of ischemically injured renal tubules. *J Cell Mol Med.* 2014; 18: 1144–56.
 20. **Popescu LM, Curici A, Wang E, et al.** Telocytes and putative stem cells in ageing human heart. *J Cell Mol Med.* 2015; 19: 31–45.
 21. **Cismasiu VB, Popescu LM.** Telocytes transfer extracellular vesicles loaded with microRNAs to stem cells. *J Cell Mol Med.* 2015; 19: 351–8.
 22. **Cretoiu SM, Radu BM, Banciu A, et al.** Isolated human uterine telocytes: immunocytochemistry and electrophysiology of T-type calcium channels. *Histochem Cell Biol.* 2015; 143: 83–94.
 23. **Roatesi I, Radu BM, Cretoiu D, et al.** Uterine telocytes: a review of current knowledge. *Biol Reprod.* 2015; doi: 10.1095/biolreprod.114.125906
 24. **Ceafalan L, Gherghiceanu M, Popescu LM, et al.** Telocytes in human skin—are they involved in skin regeneration? *J Cell Mol Med.* 2012; 16: 1405–20.
 25. **Rusu MC, Mirancea N, Manoiu VS, et al.** Skin telocytes. *Ann Anat.* 2012; 194: 359–67.
 26. **Mirancea N, Morosanu AM, Mirancea GV, et al.** Infrastructure of the telocytes from tumor stroma in the skin basal and squamous cell carcinomas. *Rom J Morphol Embryol.* 2013; 54: 1025–37.
 27. **Bek-Thomsen M, Lomholt HB, Scavenius C, et al.** Proteome analysis of human sebaceous follicle infundibula extracted from healthy and acne-affected skin. *PLoS ONE.* 2014; 9: e107908.
 28. **Manetti M, Guiducci S, Ruffo M, et al.** Evidence for progressive reduction and loss of telocytes in the dermal cellular network of systemic sclerosis. *J Cell Mol Med.* 2013; 17: 482–96.
 29. **Kanji S, Das M, Aggarwal R, et al.** Nanofiber-expanded human umbilical cord blood-derived CD34(+) cell therapy accelerates cutaneous wound closure in NOD/SCID mice. *J Cell Mol Med.* 2014; 18: 685–97.
 30. **Manetti M, Rosa I, Messerini L, et al.** A loss of telocytes accompanies fibrosis of multiple organs in systemic sclerosis. *J Cell Mol Med.* 2014; 18: 253–62.
 31. **Ho YY, Lagares D, Tager AM, et al.** Fibrosis—a lethal component of systemic sclerosis. *Nat Rev Rheumatol.* 2014; 10: 390–402.
 32. **Manetti M, Rosa I, Messerini L, et al.** Telocytes are reduced during fibrotic remodelling of the colonic wall in ulcerative colitis. *J Cell Mol Med.* 2015; 19: 62–73.
 33. **Zhong A, Wang G, Yang J, et al.** Stromal-epithelial cell interactions and alteration of branching morphogenesis in macromastitic mammary glands. *J Cell Mol Med.* 2014; 18: 1257–66.
 34. **Barsotti S, Bellando Randone S, Guiducci S, et al.** Systemic sclerosis: a critical digest of the recent literature. *Clin Exp Rheumatol.* 2014; 32: S194–205.
 35. **Li LC, Gao J, Li J.** Emerging role of HMGB1 in fibrotic diseases. *J Cell Mol Med.* 2014; 18: 2331–9.
 36. **Sheng J, Shim W, Lu J, et al.** Electrophysiology of human cardiac atrial and ventricular telocytes. *J Cell Mol Med.* 2014; 18: 355–62.
 37. **Xiao J.** Cardiac telocytes and fibroblasts in primary culture: different morphologies and immunophenotypes. *PLoS ONE.* 2015; doi:10.1371/journal.pone.0115991.
 38. **Cretoiu SM, Cretoiu D, Popescu LM.** Human myometrium - the ultrastructural 3D network of telocytes. *J Cell Mol Med.* 2012; 16: 2844–9.
 39. **Cismasiu VB, Radu E, Popescu LM.** miR-193 expression differentiates telocytes from other stromal cells. *J Cell Mol Med.* 2011; 15: 1071–4.
 40. **Zheng Y, Zhang M, Qian M, et al.** Genetic comparison of mouse lung telocytes with mesenchymal stem cells and fibroblasts. *J Cell Mol Med.* 2013; 17: 567–77.
 41. **Sun X, Zheng M, Zhang M, et al.** Differences in the expression of chromosome 1 genes between lung telocytes and other cells: mesenchymal stem cells, fibroblasts, alveolar type II cells, airway epithelial cells and lymphocytes. *J Cell Mol Med.* 2014; 18: 801–10.
 42. **Zheng M, Sun X, Zhang M, et al.** Variations of chromosomes 2 and 3 gene expression profiles among pulmonary telocytes, pneumocytes, airway cells, mesenchymal stem cells and lymphocytes. *J Cell Mol Med.* 2014; 18: 2044–60.
 43. **Zheng Y, Cretoiu D, Yan G, et al.** Comparative proteomic analysis of human lung telocytes with fibroblasts. *J Cell Mol Med.* 2014; 18: 568–89.
 44. **Kizilyaprak C, Bittermann AG, Daraspe J, et al.** FIB-SEM tomography in biology. *Methods Mol Biol.* 2014; 1117: 541–58.
 45. **Kizilyaprak C, Longo G, Daraspe J, et al.** Investigation of resins suitable for the preparation of biological sample for 3-D electron microscopy. *J Struct Biol.* 2015; 189: 135–46.
 46. **Kanazawa T, Gotoh M, Ohta K, et al.** Novel characteristics of normal supraspinatus insertion in rats: an ultrastructural analysis using three-dimensional reconstruction using focused ion beam/scanning electron microscope tomography. *Muscles Ligaments Tendons J.* 2014; 4: 182–7.

47. **Ohta K, Okayama S, Togo A, et al.** Three-dimensional organization of the endoplasmic reticulum membrane around the mitochondrial constriction site in mammalian cells revealed by using focused-ion beam tomography. *Microscopy*. 2014; 63: i34.
48. **Narayan K, Danielson CM, Lagarec K, et al.** Multi-resolution correlative focused ion beam scanning electron microscopy: applications to cell biology. *J Struct Biol*. 2014; 185: 278–84.
49. **Pham TT, Maenz S, Ludecke C, et al.** Quantitative characterization of endothelial cell morphologies depending on shear stress in different blood vessels of domestic pigs using a focused ion beam and high resolution scanning electron microscopy (FIB-SEM). *Tissue Cell*. 2014; doi:10.1016/j.tice.2014.12.005.
50. **Sonomura T, Furuta T, Nakatani I, et al.** Attempt of correlative observation of morphological synaptic connectivity by combining confocal laser-scanning microscope and FIB-SEM for immunohistochemical staining technique. *Microscopy*. 2014; 63: i8.
51. **Kubota Y.** New developments in electron microscopy for serial image acquisition of neuronal profiles. *Microscopy*. 2015; 64: 27–36.
52. **Kizilyaprak C, Daraspe J, Humbel BM.** Focused ion beam scanning electron microscopy in biology. *J Microsc*. 2014; 254: 109–14.
53. **Mourik MJ, Faas FG, Zimmermann H, et al.** Towards the imaging of Weibel-Palade body biogenesis by serial block face-scanning electron microscopy. *J Microsc*. 2015; doi:10.1111/jmi.12222.
54. **Niculite CM, Regalia TM, Gherghiceanu M, et al.** Dynamics of telopodes (telocyte prolongations) in cell culture depends on extracellular matrix protein. *Mol Cell Biochem*. 2015; 398: 157–64.
55. **Campeanu RA, Radu BM, Cretoiu SM, et al.** Near-infrared low-level laser stimulation of telocytes from human myometrium. *Lasers Med Sci*. 2014; 29: 1867–74.
56. **Fertig ET, Gherghiceanu M, Popescu LM.** Extracellular vesicles release by cardiac telocytes: electron microscopy and electron tomography. *J Cell Mol Med*. 2014; 18: 1938–43.
57. **Raposo G, Stoorvogel W.** Extracellular vesicles: exosomes, microvesicles, and friends. *J Cell Biol*. 2013; 200: 373–83.
58. **Lotvall J, Hill AF, Hochberg F, et al.** Minimal experimental requirements for definition of extracellular vesicles and their functions: a position statement from the International Society for Extracellular Vesicles. *J Extracell Vesicles*. 2014; 3: 26913.
59. **Popescu LM, Manole E, Serboiu CS, et al.** Identification of telocytes in skeletal muscle interstitium: implication for muscle regeneration. *J Cell Mol Med*. 2011; 15: 1379–92.
60. **De Jong OG, Van Balkom BW, Schiffelers RM, et al.** Extracellular vesicles: potential roles in regenerative medicine. *Front Immunol*. 2014; 5: 608.
61. **Smythies J, Edelstein L.** Telocytes, exosomes, gap junctions and the cytoskeleton: the makings of a primitive nervous system? *Front Cell Neurosci*. 2014; 7: 278.
62. **Edelstein L, Smythies J.** The role of telocytes in morphogenetic bioelectrical signaling: once more unto the breach. *Front Mol Neurosci*. 2014; 7: 41.
63. **Kornberg TB.** Cytonemes and the dispersion of morphogens. *Wiley Interdiscip Rev Dev Biol*. 2014; 3: 445–63.
64. **Haines DD, Juhasz B, Tosaki A.** Management of multicellular senescence and oxidative stress. *J Cell Mol Med*. 2013; 17: 936–57.